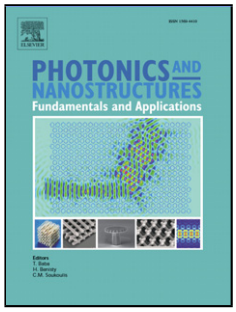

Title: Multiscale Methods for Engineering Double Negative Metamaterials

Author: Yue Chen Robert Lipton

PII: S1569-4410(13)00046-1
DOI: http://dx.doi.org/doi:10.1016/j.photonics.2013.07.005
Reference: PNFA 405

To appear in: *Photonics and Nanostructures – Fundamentals and Applications*

Received date: 18-12-2012
Revised date: 27-5-2013
Accepted date: 28-5-2013

Please cite this article as: Yue Chen, Robert Lipton, Multiscale Methods for Engineering Double Negative Metamaterials, *Photonics and Nanostructures - Fundamentals and Applications* (2013), http://dx.doi.org/10.1016/j.photonics.2013.07.005

Multiscale Methods for Engineering Double Negative Metamaterials

Yue Chen
Department of Mathematics
University of Kentucky
Lexington, KY 40506, USA.
email: chenyue0715@uky.edu

Robert Lipton
Department of Mathematics
Louisiana State University
Baton Rouge, LA 70803, USA.
email: lipton@math.lsu.edu

May 27, 2013

Abstract

Key words: Metamaterial, dispersion relation, dissipative media

The approach taken here solves the Maxwell equations inside metamaterial crystals directly and explicitly with no approximations made. The Bloch wave solution and dispersion relation is given by a power series in the ratio between wave number and period. Each term is iteratively defined by the solution of an auxiliary problem depending on the configuration and shapes of the scatterers. The leading order term in the power series for the dispersion relation is given by the complex effective index of refraction. The effective properties and their resonance frequencies depend explicitly on the shape of the scatterers. Double negative behavior is explicitly controlled by the location of resonance frequencies related to spectra intrinsic to the geometric configuration of the multi-phase inclusions. This provides for the rational shape design of inclusions for control of double negative behavior across prescribed frequency ranges.

1 Introduction

A compelling aspect of metamaterials research is the quest for new sub-wavelength microstructures that deliver both negative bulk dielectric constant and bulk magnetic permeability across prescribed frequency intervals. Double negative materials offer great potential for applications in biomedical imaging, optical lithography and data storage. Such media support electromagnetic waves for which the phase velocity is antiparallel to the direction of energy flow as well as other unusual electromagnetic effects such as the reversal of the Doppler effect and Cerenkov radiation [41].

Double negative metamaterials are characterized by sub-wavelength microstructure and control radiation through a delicate combination of local and global resonances. This approach to controlling wave propagation is distinct from approaches using photonic materials which control radiation through multiple diffraction implemented by structuring the medium along the same length scale as the wave length of the incident radiation. Pendry [29] demonstrated that unconventional properties can be derived from sub-wavelength configurations of different conventional materials. It was shown that a cubic lattice of metal wires exhibited behavior associated with negative bulk dielectric constant near the plasma resonance of the structure. This resonance frequency is intrinsic to the lattice and lies in the microwave regime six decades below the plasma resonance of the metal used to make the lattice. Subsequently non-magnetic metallic split-ring resonators were constructed to deliver negative effective magnetic permeability at microwave frequencies [28]. In more recent work Smith et al. [39] experimentally demonstrated that arrays of metallic posts and split ring resonators could

also support resonances at microwave frequencies and deliver negative effective negative refractive index for a range of microwave frequencies. Subsequent work has delivered several new configurations of metallic resonators for double negative behavior [15, 19, 34, 46, 47, 48]. New designs for generating double negative properties in the optical regime rely on Mie resonances. One scheme employs coated rods made from a high dielectric core coated with a frequency dependent dielectric plasmonic or Drude type behavior at optical frequencies [43, 44, 45]. Other schemes employ small particles made from dielectric materials with large permittivity, [20, 30, 42]. Alternate strategies for generating negative bulk dielectric permeability at infrared and optical frequencies use special configurations of plasmonic nanoparticles [1], [37]. The list of metamaterial designs continues to grow and recent reviews of the subject can be found in [32] and [33].

In this article we focus on a class of simple microstructures and investigate the range of double negative behavior that one can engineer using lossy nonmagnetic materials. The main point of the article is to introduce a multi-scale method for exploring the universe of sub-wavelength microstructures that links the geometry of the microstructure to the actual dispersion relations for the medium without making use of any simplifying approximation (e.g. the dipole approximation). Here we consider periodic arrays of nonmagnetic scatterers made from two distinct materials. We present a systematic method for recovery of the band structure of the metamaterial. Each branch of the dispersion relation is given by power series in the ratio of period to wave number. The leading order term in the expansion is the effective complex index of refraction for the medium. Figures displaying the real and imaginary parts of the leading order dispersion relation for several different bands are displayed in section 3 see, Figures 4(a) through 4(d). The higher order terms in the series involve corrections for spatial dispersion. When the media is assumed lossless the power series for each branch is shown to converge, see [12]. This is also true for lossy materials. This expansion provides the rigorous and explicit connection between microgeometry and dispersion. It provides the opportunity for the systematic design of sub-wavelength structures for control of dispersion based on the shape and topology of the inclusions used in the microgeometry. This is taken up in section 3 where several simulations exhibiting the sensitivity of the dispersion relations to the underlying geometry of the scatterers is presented. The methodology provides a way to systematically identify the location of the center frequency and band width of double negative intervals through calculation of auxiliary spectral problems intrinsic to the geometry. Table 1 of section 3 illustrates how the center frequency and band width of a preselected double negative interval can be adjusted by changing the geometry of the scatterer. This methodology presented here is a multiscale approach in that the Maxwell equations are solved exactly in terms of a power series that has as its expansion parameter the ratio between the crystal period and the wave number. When the expansion parameter is small and the crystal period is *subwavelength* the leading order terms in the dispersion relation control the physics. For larger values of the expansion parameter when the crystal period is closer to the wavelength of propagation the higher order terms in the series become important in describing nonlocal effects such as spatial dispersion.

To demonstrate the method we construct metamaterials made from sub-wavelength periodic arrangements of nonmagnetic infinitely long parallel coated cylinders immersed in a nonmagnetic host. In what follows the period of the lattice is denoted by d. The coated cylinders are parallel to the x_3 axis and made from a frequency independent high dielectric core and a frequency dependent dielectric plasmonic coating (Figure 1). The host medium containing the coated rods has relative dielectric permittivity equal to unity. To generate effective magnetic properties the material comprising the core of the rod is chosen to be a high contrast dielectric material $\epsilon_R = \gamma/d^2$ see, [9]. The dielectric coating is frequency dependent and characterized by single oscillator model that includes dissipation.

The approach taken here solves the Maxwell equations directly and explicitly with no approximations made. The solution is given by a power series with each term iteratively defined by the solution of an auxiliary problem that is simpler than the original Maxwell system. In what follows we apply the power series method to identify the dispersion relation for TE modes with magnetic field parallel to the cylinders. The leading order term in the power series for the dispersion relation is given by

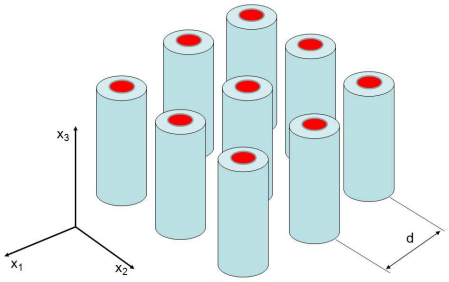

Figure 1: Periodic array of coated dielectric rods with period d

the complex effective index of refraction expressed in terms of the effective magnetic permeability and effective dielectric permittivity tensor. These tensors are seen to resonate at frequencies related to spectra intrinsic to the cross-sectional shape and configuration of the coated rods. It is the interlacing of the eigenvalues associated with two distinct spectra that determine frequency intervals over which double negative behavior occur. The first spectra identified by the power series method is the Dirichlet spectra of the cross-sectional shape of the rod core. This spectra is local and depends only on the shape of each rod core. The second spectra is a type of electrostatic spectra associated with a three phase medium and is global and intrinsic to the structural geometry. This spectra is associated with the configuration of the periodic structure and the relative position of the scatterers with respect to each other. Both spectral problems emerge naturally from the power series method and are not part of any imposed hypotheses. Electrostatic spectra for two phase materials has been recognized as useful in characterizing electromagnetic properties of periodic nano structures see, for example [37]. Earlier pioneering work [4], [23], identified electrostatic modes and showed how their use allows for the separation of the dielectric properties of the component materials from underlying geometric effects due to the structure of two-phase composites. Numerical methods for computation of electrostatic spectra for complex two-phase structures are developed in [24]

For the problem at hand we apply the strategy developed by the authors in [12] and [11] to express the complex effective dielectric constant in terms of a new type of three phase electrostatic spectra. The effective dielectric constant is expressed in a spectral representation formula that explicitly links the configuration of the scatters to effective properties. Similarly the Dirichlet spectra delivers a representation formula for the magnetic permittivity. This formula agrees with the representation formula for the magnetic permittivity developed in the work of [9] for periodic arrays of high dielectric rods. In this article we provide explicit power series for the associated Bloch wave solutions and dispersion relations. The full details of all higher order boundary value problems can be found in [12], [11]. We apply the power series representation to calculate the average Poynting vector to show that in the homogenization limit the energy flow and phase velocity are in opposite directions over frequency intervals associated with double negative behavior. We also point out that the double negative behavior is not the necessary and sufficient condition for the energy flow to be opposite to the phase velocity and identify necessary and sufficient conditions for which it is so see, section 4. We compute center frequency and bandwidth of double negative intervals for several choices of inner and outer radii of the rod coating and compare these with the dispersion curves for the imaginary part of the wave number versus frequency. From this we can identify which design delivers a double negative interval associated with the least attenuation of average electromagnetic energy flow (4.3) see, Figure 4 of section 3 and the following discussion.

We conclude the introduction noting that formulas for frequency-dependent effective magnetic permeability together with conditions for generation of negative effective permeability are developed in [7, 8, 9, 14, 16, 21]. For periodic arrays made from metal fibers a homogenization theory delivering negative effective dielectric constant [6] has been established. A novel method for creating metamaterials with prescribed effective dielectric permittivity and effective magnetic permeability

at a fixed frequency is developed in [26]. New methodologies and issues for computing homogenized properties for metamaterials using top down approaches are presented in [2], [3], [38]. Earlier work on the power series approach to sub-wavelength analysis has been developed and applied in [17] for characterizing the dynamic dispersion relations for Bloch waves inside plasmonic crystals. It has also been applied to assess the influence of effective negative permeability on the propagation of Bloch waves inside high contrast dielectrics [18], the generation of negative permeability inside metallic - dielectric resonators [36], and for concentric coated cylinder assemblages generating a double negative media [13].

2 Power series representations

We start with a metamaterial crystal characterized by a period cell containing a centered coated cylinder with plasmonic coating and high dielectric core. The core radius and the coating radius are denoted by a and b respectively (Figure 2). The cylinder is parallel to the x_3 axis and is periodically

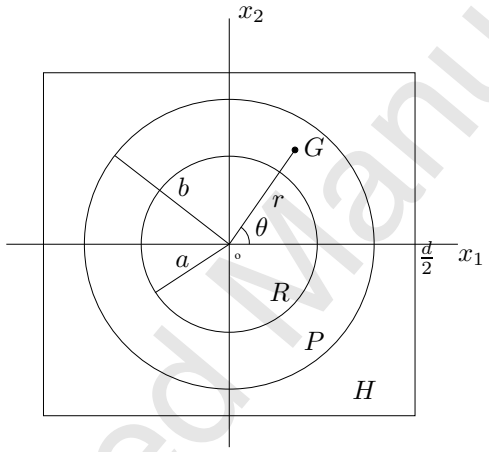

Figure 2: The period cell: R represents the high dielectric core, P the plasmonic coating and H denotes the connected host material.

arranged within a square lattice over the transverse $\mathbf{x} = (x_1, x_2)$ plane. The period of the lattice is denoted by d. For TE-polarized Bloch-waves, the magnetic field is aligned with the cylinders and the electric field lies in the transverse plane. The direction of propagation is described by the unit vector $\hat{\kappa} = (\kappa_1, \kappa_2)$ and $k \in \mathbb{C}$ is the complex wave number and the fields are of the form

$$H_3 = H_3(\mathbf{x})e^{i(k\hat{\kappa}\cdot\mathbf{x}-t\omega)},\ E_1 = E_1(\mathbf{x})e^{i(k\hat{\kappa}\cdot\mathbf{x}-t\omega)},\ E_2 = E_2(\mathbf{x})e^{i(k\hat{\kappa}\cdot\mathbf{x}-t\omega)} \tag{2.1}$$

where $H_3(\mathbf{x})$, $E_1(\mathbf{x})$, and $E_2(\mathbf{x})$ are d-periodic for $\mathbf{x}$ in $\mathbb{R}^2$. Here c denotes the speed of light in free space. We denote the unit vector pointing along the x_3 direction by $\mathbf{e}_3$, and the periodic dielectric permittivity and magnetic permeability are denoted by a_d and μ respectively. The electric field component $\mathbf{E} = (E_1, E_2)$ of the wave is determined by

$$\mathbf{E} = -\frac{ic}{\omega a_d}\mathbf{e}_3 \times \nabla H_3. \tag{2.2}$$

The materials are assumed non-magnetic hence the magnetic permeability μ is set to unity inside the coated cylinder and host. The oscillating dielectric permittivity for the crystal is a d periodic function in the transverse plane and is described by $a_d = a_d(\mathbf{x}/d)$ where $a_d(\mathbf{y})$ is the unit periodic

dielectric function taking the values

$$a_d(\mathbf{y}) = \begin{cases} \epsilon_H & \text{in the host material,} \\ \epsilon_P(\omega) & \text{in the frequency dependent "plasmonic" coating,} \\ \epsilon_R = \gamma/d^2 & \text{in the high dielectric core.} \end{cases} \tag{2.3}$$

Here γ in a complex number and has dimensions of area and the frequency dependent permittivity ϵ_P of the plasmonic coating is given by

$$\epsilon_P(\omega) = 1 - \frac{\omega_p^2}{\omega^2 + i\omega_c\omega}, \tag{2.4}$$

where the paramaters are the incident frequency ω, the damping constant ω_c and the plasma frequency ω_p. Setting $h^d(\mathbf{x}) = H_3(\mathbf{x})e^{i(k\hat{\kappa}\cdot\mathbf{x})}$ the Maxwell equations take the form of the Helmholtz equation given by

$$-\nabla_{\mathbf{x}} \cdot \left(a_d^{-1}(\frac{\mathbf{x}}{d})\nabla_{\mathbf{x}} h^d(\mathbf{x})\right) = \frac{\omega^2}{c^2} h^d \quad \text{in } \mathbb{R}^2. \tag{2.5}$$

We set $\mathbf{x} = d\mathbf{y}$ for $\mathbf{y}$ inside the unit period $Y = [-0.5, 0.5]^2$, put $\beta = dk\hat{\kappa}$ and write $u(\mathbf{y}) = H_3(d\mathbf{y})$. The dependent variable is written $u^d(\mathbf{y}) = h^d(d\mathbf{y}) = u(\mathbf{y})\exp^{i\beta\cdot\mathbf{y}}$, and we recover the equivalent problem over the unit period cell given by

$$-\nabla_{\mathbf{y}} \cdot \left(a_d^{-1}(\mathbf{y})\nabla_{\mathbf{y}} u^d\right) = \frac{d^2\omega^2}{c^2} u^d \quad \text{in } Y. \tag{2.6}$$

We start by introducing the power series in terms of the ratio of period size to wavelength $\eta = dk$ and frequency $\xi = \frac{\omega}{kc}$.

For these parameters the dielectric permittivity in the coating takes the value $\epsilon_P(\xi k) = 1 - \frac{\omega_p^2/c^2}{(\xi k)^2 + i(\omega_c/c)(\xi k)}$, and (2.6) is given by

$$-\nabla_{\mathbf{y}} \cdot \left(a_d^{-1}(\mathbf{y})\nabla_{\mathbf{y}} u^d(\mathbf{y})\right) = \eta^2\xi^2 u^d(\mathbf{y}) \quad \text{in } Y. \tag{2.7}$$

The unit period cell for the generic metamaterial system is represented in Figure 2. In what follows R represents the rod core cross section containing high dielectric material, P the coating containing the plasmonic material and H denotes the connected host material. The jump conditions implied by (2.7) are given by

$$n \cdot \nabla_{\mathbf{y}} u^d_{|_H} = n \cdot \epsilon_P^{-1}(\xi k) n \cdot \nabla_{\mathbf{y}} u^d_{|_P}, \text{ H-P interface,} \tag{2.8}$$

$$n \cdot \epsilon_P^{-1}(\xi k)\nabla_{\mathbf{y}} u^d_{|_P} = n \cdot \frac{d^2}{\gamma}\nabla_{\mathbf{y}} u^d_{|_R}, \text{R-P interface.} \tag{2.9}$$

Here "H-P" interface denotes the interface separating host from the plasmonic coating and "R-P" interface denotes the interface separating the rod core material and the plasmonic coating and n denotes the normal vectors pointing from the core into the coating on the "R-P" interface and the coating into the host on the "H-P" interface.

Expanding the Bloch wave u^d eigenvalue ξ pair in power series

$$u^d = \underline{u}_0 \sum_{m=0}^{\infty} \eta^m i^m \psi_m e^{i\hat{\kappa}\cdot\tau\rho\mathbf{y}} \tag{2.10}$$

$$\xi = \sum_{m=0}^{\infty} \eta^m \xi_m \tag{2.11}$$

and substitution of (2.10) and (2.11) into (2.7), (2.8), (2.9) we equate like powers of η to identify the boundary value problem satisfied by each term in the power series. Here $\underline{u}_0$ is an arbitrary constant factor appearing in front of the sum (2.10). The leading order dispersion relation is given by

$$\xi_0^2 = n_{eff}^{-2}(\xi_0 k), \tag{2.12}$$

where the complex effective index of diffraction n_{eff}^2 depends upon the direction of propagation $\hat{\kappa}$ and is written

$$n_{eff}^2(\xi_0 k) = \mu_{eff}(\xi_0 k)/\epsilon_{eff}^{-1}(\xi_0 k)\hat{\kappa}\cdot\hat{\kappa}. \tag{2.13}$$

The frequency dependent complex effective magnetic permeability μ_{eff} and complex effective dielectric permittivity ϵ_{eff} are given by

$$\mu_{eff}(\xi_0) = \int_Y \psi_0 = \theta_H + \theta_P + \sum_{n=1}^{\infty} \frac{\mu_n < \phi_n >_R^2}{\mu_n - \gamma k^2 \xi_0^2} \tag{2.14}$$

and

$$\begin{aligned} \epsilon_{eff}^{-1}(\xi_0)\hat{\kappa}\cdot\hat{\kappa} &= \int_{Y\setminus R} a_d^{-1}(y)(\nabla\psi_1 + \hat{\kappa})\cdot\hat{\kappa}\, dy \\ &= \theta_H + \epsilon_P^{-1}(\xi_0 k)\theta_P \\ &\quad - \sum_{-1/2<\lambda_h<1/2} \left(\frac{|\alpha_{\lambda_h}^{(1)}|^2 + 2\epsilon_P^{-1}(\xi_0 k)\alpha_{\lambda_h}^{(1)}\alpha_{\lambda_h}^{(2)} + \epsilon_P^{-2}(\xi_0 k)|\alpha_{\lambda_h}^{(2)}|^2}{1 + (\epsilon_P^{-1}(\xi_0 k) - 1)(\frac{1}{2} - \lambda_h)} \right), \end{aligned} \tag{2.15}$$

where θ_H and θ_P are the areas occupied by regions H and P respectively. The magnetic Bloch wave solution of (2.5) is given by

$$H_3 = \underline{u}_0 \left(\psi_0(\mathbf{x}/d) + \sum_{l=1}^{\infty} (\tau\rho)^l i^l \psi_l(\mathbf{x}/d) \right) \exp\left\{ i\left(k\hat{\kappa}\cdot\mathbf{x} - t\omega\right)\right\}. \tag{2.16}$$

These expansions and leading order dispersion relations are found following the methods developed in [12]. The poles μ_n of the effective magnetic permeability function (2.14) are given by the Mie resonances of the rod core which for this case are given by the Dirichlet spectrum of the core cross section. The poles λ_h of the effective dielectric permittivity function (2.15) occur at the electrostatic resonances (also known as plasmon resonances) of the structure. For a lattice of period d the power series representation applies and the leading order dispersion relation dominates provided that the dielectric constant ϵ_R in the rod core is large and on the order of $1/d^2$.

From a physical perspective the plasmon resonances are associated with source free fields. These resonances occur at frequencies for which free-space wavelengths are large in comparison with the transverse dimension of the rods, i.e., $|\eta| = |kd| < 1$. For this case the time harmonic electromagnetic fields surrounding the coated rod and within the coating vary almost with the same phase. Hence at any instant of time these fields appear to be electrostatic. When the dielectric permittivity of the metallic coating is negative, source-free electrostatic fields will appear within the coating and in the region surrounding the rods. It is these electrostatic resonances or plasmons that provide the poles of the effective dielectric permittivity function. Here the electrostatic resonances can occur only in media with dispersive dielectric properties for which the real part of the dielectric permittivity assumes negative values for some range of frequencies. For the metal coating used here, this frequency range is below the plasma frequency given by the Drude model (2.4).

3 Dispersion curves

In this section, we recover leading order behavior for the dispersive behavior of the metamaterial for periods with finite size $d > 0$. To proceed we fix $d = c/\omega_p$. In these variables the power series expansion for the dispersion relation is given by

$$\left(\frac{\omega}{\omega_p}\right)^2 = \left(\frac{\omega_0}{\omega_p}\right)^2 + \sum_{l=1}^{\infty} (dk)^l \left(\frac{\omega_l}{\omega_p}\right)^2, \tag{3.1}$$

where higher order terms ω_l are functions of ω_0. To leading order the dispersion relation is given by [12], [11],

$$(dk)^2 = \left(\frac{\omega_0}{\omega_p}\right)^2 n_{eff}^2 \tag{3.2}$$

where the complex effective refractive index n_{eff} depends on the direction of propagation $\hat{\kappa}$ and normalized frequency $\frac{\omega_0}{\omega_p}$ and is given by

$$n_{eff}^2 = \mu_{eff}(\frac{\omega_0}{\omega_p})/(\epsilon_{eff}^{-1}(\frac{\omega_0}{\omega_p})\hat{\kappa}\cdot\hat{\kappa}). \tag{3.3}$$

Note that $dk = dk_r + idk_i$ where k_r and k_i are the real and imaginary parts of k.

With this choice we can write out the real and imaginary parts of μ_{eff} explicitly as follows

$$Re(\mu_{eff}) = \theta_H + \theta_P + \sum_{n=1}^{\infty} \frac{\mu_n < \phi_n >_R^2 (\epsilon'_R\mu_n - \epsilon'_R(\frac{\omega_0}{\omega_p})^2)}{\mu_n^2 - 2\mu_n\epsilon'_R(\frac{\omega_0}{\omega_p})^2 + |\epsilon_R|^2(\frac{\omega_0}{\omega_p})^4} \tag{3.4}$$

and

$$Im(\mu_{eff}) = \sum_{n=1}^{\infty} \frac{\mu_n < \phi_n >_R^2 \epsilon''_R(\frac{\omega_0}{\omega_p})^2}{\mu_n^2 - 2\mu_n\epsilon'_R(\frac{\omega_0}{\omega_p})^2 + |\epsilon_R|^2(\frac{\omega_0}{\omega_p})^4} \tag{3.5}$$

where $\epsilon_R = \epsilon'_R + i\epsilon''_R$. Before writing out the real and imaginary parts of $\epsilon_{eff}^{-1}\hat{\kappa}\cdot\hat{\kappa}$, for convenience, we set

$$\begin{aligned}
A_h &= \left(\left((\frac{\omega_0}{\omega_p})^2 - 1\right)^2 - (\frac{\omega_c}{\omega_p})^2(\frac{\omega_0}{\omega_p})^2\right)|\alpha_{\lambda_h}^{(1)}|^2 + 2(\frac{\omega_0}{\omega_p})^2\left((\frac{\omega_0}{\omega_p})^2 - (\frac{\omega_c}{\omega_p})^2 - 1\right)\alpha_{\lambda_h}^{(1)}\alpha_{\lambda_h}^{(2)} \\
&\quad +(\frac{\omega_0}{\omega_p})^2\left((\frac{\omega_0}{\omega_p})^2 - (\frac{\omega_c}{\omega_p})^2\right)|\alpha_{\lambda_h}^{(2)}|^2, \\
B_h &= 2(\frac{\omega_c}{\omega_p})(\frac{\omega_0}{\omega_p})\left((\frac{\omega_0}{\omega_p})^2 - 1\right)|\alpha_{\lambda_h}^{(1)}|^2 + 2(\frac{\omega_c}{\omega_p})(\frac{\omega_0}{\omega_p})\left(2(\frac{\omega_0}{\omega_p})^2 - 1\right)\alpha_{\lambda_h}^{(1)}\alpha_{\lambda_h}^{(2)} \\
&\quad +2(\frac{\omega_c}{\omega_p})(\frac{\omega_0}{\omega_p})^3|\alpha_{\lambda_h}^{(2)}|^2, \\
C_h &= \left((\frac{\omega_0}{\omega_p})^2 - 1\right)^2 - (\frac{\omega_c}{\omega_p})^2(\frac{\omega_0}{\omega_p})^2 + (\frac{1}{2} - \lambda_h)\left((\frac{\omega_0}{\omega_p})^2 - 1\right), \\
D_h &= 2(\frac{\omega_c}{\omega_p})(\frac{\omega_0}{\omega_p})\left((\frac{\omega_0}{\omega_p})^2 - 1\right) + (\frac{1}{2} - \lambda_h)(\frac{\omega_c}{\omega_p})(\frac{\omega_0}{\omega_p}).
\end{aligned}$$

Then the real and imaginary parts of $\epsilon_{eff}^{-1}\hat{\kappa}\cdot\hat{\kappa}$ are given by

$$Re(\epsilon_{eff}^{-1}\hat{\kappa}\cdot\hat{\kappa}) = \theta_H + \frac{(\frac{\omega_0}{\omega_p})^2\left((\frac{\omega_0}{\omega_p})^2 + (\frac{\omega_c}{\omega_p})^2 - 1\right)}{\left((\frac{\omega_0}{\omega_p})^2 - 1\right) + (\frac{\omega_c}{\omega_p})^2(\frac{\omega_0}{\omega_p})^2}\theta_P - \sum_{-1/2<\lambda_h<1/2} \frac{A_hC_h + B_hD_h}{C_h^2 + D_h^2} \tag{3.6}$$

and

$$Im(\epsilon_{eff}^{-1}\hat{\kappa}\cdot\hat{\kappa}) = -\frac{(\frac{\omega_c}{\omega_p})(\frac{\omega_0}{\omega_p})}{\left((\frac{\omega_0}{\omega_p})^2 - 1\right) + (\frac{\omega_c}{\omega_p})^2(\frac{\omega_0}{\omega_p})^2}\theta_P + \sum_{-1/2<\lambda_h<1/2} \frac{A_hD_h - B_hC_h}{C_h^2 + D_h^2}. \tag{3.7}$$

Table 1 shows the changes of the double negative interval when inner radius and outer radius vary. In each cell, the upper number denotes the length of the frequency interval where both real

	$a = 0.5b$	$a = 0.55b$	$a = 0.6b$	$a = 0.65b$
b=0.3	0	0	0	0.0332 (0.8919)
b=0.35	0	0.02733 (0.9003)	0.03824 (0.8315)	0.04425 (0.7716)
b=0.4	0.03541 (0.8707)	0.04204 (0.7960)	0.04893 (0.7345)	0.05579 (0.6830)
b=0.45	0.04366 (0.7795)	0.05143 (0.7141)	0.05944 (0.6605)	0.06801 (0.6161)

Table 1: The changes of the double negative interval when inner radius and outer radius vary. In each cell, the upper number denotes the length of the interval where both real parts of μ_{eff} and $\epsilon_{eff}^{-1}\hat{\kappa}\cdot\hat{\kappa}$ are negative. The lower number shows the center value of $\frac{\omega_0}{\omega_p}$ in the double negative interval.

parts of μ_{eff} and $\epsilon_{eff}^{-1}\hat{\kappa}\cdot\hat{\kappa}$ are negative. The lower number shows the center value of $\frac{\omega_0}{\omega_p}$ in the double negative interval. Figure 3 shows the real and imaginary parts of μ_{eff} and $\epsilon_{eff}^{-1}\hat{\kappa}\cdot\hat{\kappa}$ associated with different choice of inner radius a and outer radius b when $\epsilon_R = 200 + i5$ and $\omega_c/\omega_p = 0.01$. Here $Im(\epsilon_{eff}^{-1}\hat{\kappa}\cdot\hat{\kappa}) \leq 0$ and the imaginary part of the effective dielectric constant ϵ_i given by (4.5) is positive. The green strip gives the interval in which both real parts of μ_{eff} and ϵ_{eff} are negative. (a) is for the case $a = 0.5b, b = 0.4$, (b) for $a = 0.6b, b = 0.4$, and (c) for $a = 0.5b, b = 0.45$, and (d) for $a = 0.65b, b = 0.45$. It highlights the changes of the double negative interval with respect to the change in the inner and outer radii of the coating. Figure 4 shows the dispersion curves associated with different choices of inner radius a and outer radius b when, $\epsilon_R = 200+i5$ and $\omega_c/\omega_p = 0.01$. The dashed line corresponds to the imaginary part dk_i while the solid line corresponds to the real part dk_r. The green strip denotes the interval where $\mu_r = Re(\mu_{eff})$ and $\epsilon_r = Re(\epsilon_{eff}^{-1}\hat{\kappa}\cdot\hat{\kappa})/|\epsilon_{eff}^{-1}\hat{\kappa}\cdot\hat{\kappa}|^2$ are both negative. (a) is for the case $a = 0.5b$, $b = 0.4$, (b) for $a = 0.6b$, $b = 0.4$, (c) for $a = 0.5b$, $b = 0.45$, and (d) for $a = 0.65b$, $b = 0.45$. From Figure 4 we see that the double negative interval associated with case (a), the inner and outer coating radii of $a = 0.5b$ and $b = 0.4$, is associated with the least attenuation of average electromagnetic energy flow (4.3) along the direction of propagation.

4 Homogenization and energy flow in the double negative regime

For TE-polarized waves, the magnetic field $\mathbf{H}(\mathbf{x}/d) = (0, 0, H_3(\mathbf{x}/d))$ where $H_3(\mathbf{x}/d)$ is given by (2.16) and the electric field $\mathbf{E}(\mathbf{x}/d) = (E_1(\mathbf{x}/d), E_2(\mathbf{x}/d), 0)$. Both fields are related through (2.2). Therefore

$$\mathbf{E}(\mathbf{x}/d) = \frac{ic}{\omega a_d}\partial_{x_2}H_3(\mathbf{x}/d)\mathbf{e_1} - \frac{ic}{\omega a_d}\partial_{x_1}H_3(\mathbf{x}/d)\mathbf{e_2}, \tag{4.1}$$

where $\mathbf{e_i}$ is the unit vector along the x_i direction for $i = 1, 2, 3$. The time average of the Poynting vector is given by

$$\begin{aligned}\mathbf{P}^d &= \frac{1}{2}Re[\mathbf{E}(\mathbf{x}/d) \times \overline{\mathbf{H}(\mathbf{x}/d)}] \\ &= \frac{1}{2}Re[E_2(\mathbf{x}/d)\overline{H_3(\mathbf{x}/d)}\mathbf{e_1} - E_1(\mathbf{x}/d)H_3(\mathbf{x}/d)\mathbf{e_2}].\end{aligned} \tag{4.2}$$

Consider any fixed averaging domain D transverse to the cylinders and the spatial average of the electromagnetic energy flow along the direction $\hat{\kappa}$ over this domain is written $\langle \mathbf{P}^d \cdot \hat{\kappa} \rangle_D$. Substituting (2.16) and (4.1) into (4.2) and taking the limit of (4.2) as $d \to 0$ shows that the average

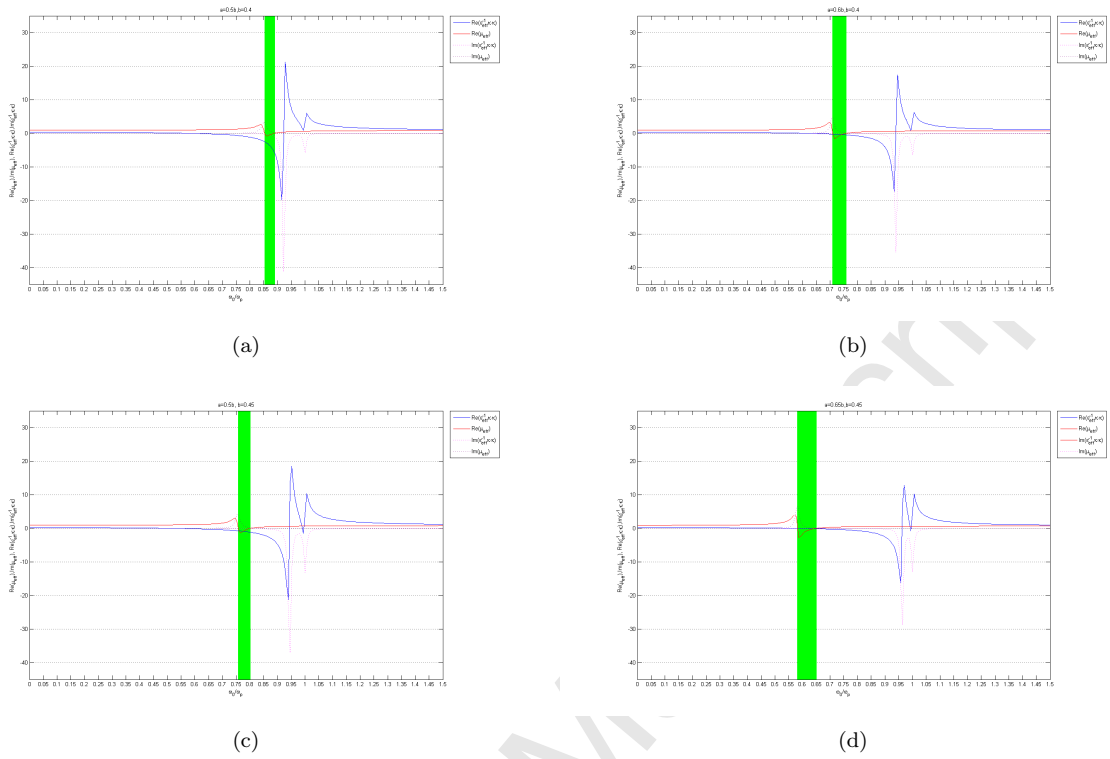

(a) (b)

(c) (d)

Figure 3: Real and imaginary part of the effective permittivity and permeability associated with different choice of inner and outer radii for the coating, when $\epsilon_R = 200 + i5$ and $\omega_c/\omega_p = 0.01$. The green strip gives the interval where the real parts of $\mu_r = \mu_{eff}$ and $\epsilon_r = \epsilon_{eff}^{-1}\hat{\kappa}\cdot\hat{\kappa}/|\epsilon_{eff}^{-1}\hat{\kappa}\cdot\hat{\kappa}|^2$ are both negative. (a) is for $a = 0.5b$, $b = 0.4$; (b) for $a = 0.6b$, $b = 0.4$; (c) for $a = 0.5b$, $b = 0.45$; (d) for $a = 0.65b$, $b = 0.45$.

electromagnetic energy flow along the direction $\hat{\kappa}$ is given by

$$\lim_{d\to 0}\langle \mathbf{P}^d\cdot\hat{\kappa}\rangle_D = Re\left(\frac{\mu_{eff}}{n_{eff}}\right)\frac{|\underline{u}_0|^2}{2}\exp(-2Im(k)\hat{\kappa}\cdot\mathbf{x}). \tag{4.3}$$

In the $d\to 0$ limit, the phase velocity of the effective medium is along the direction $\hat{\kappa}$ and determined by

$$\mathbf{v}_p = \frac{c}{Re(n_{eff})}\hat{\kappa}. \tag{4.4}$$

For future reference we denote $\mu_r = Re(\mu_{eff})$, $\mu_i = Im(\mu_{eff})$ and

$$\epsilon_r = Re(\epsilon_{eff}) = \frac{Re(\epsilon_{eff}^{-1}\hat{\kappa}\cdot\hat{\kappa})}{|\epsilon_{eff}^{-1}\hat{\kappa}\cdot\hat{\kappa}|^2}, \epsilon_i = Im(\epsilon_{eff}) = \frac{-Im(\epsilon_{eff}^{-1}\hat{\kappa}\cdot\hat{\kappa})}{|\epsilon_{eff}^{-1}\hat{\kappa}\cdot\hat{\kappa}|^2}. \tag{4.5}$$

There are two resultant complex refractive indices, $n_{eff\pm} = \pm\sqrt{\mu_{eff}\epsilon_{eff}}$ where $\mu_{eff} = \mu_r + i\mu_i$ and $\epsilon_{eff} = \epsilon_r + i\epsilon_i$. Now $n_{eff\pm}$ can be written as

$$n_{eff\pm} = \pm\sqrt{|\mu_{eff}||\epsilon_{eff}|}\exp(i\phi_n), \quad \phi_n = \frac{\phi_\epsilon + \phi_\mu}{2}. \tag{4.6}$$

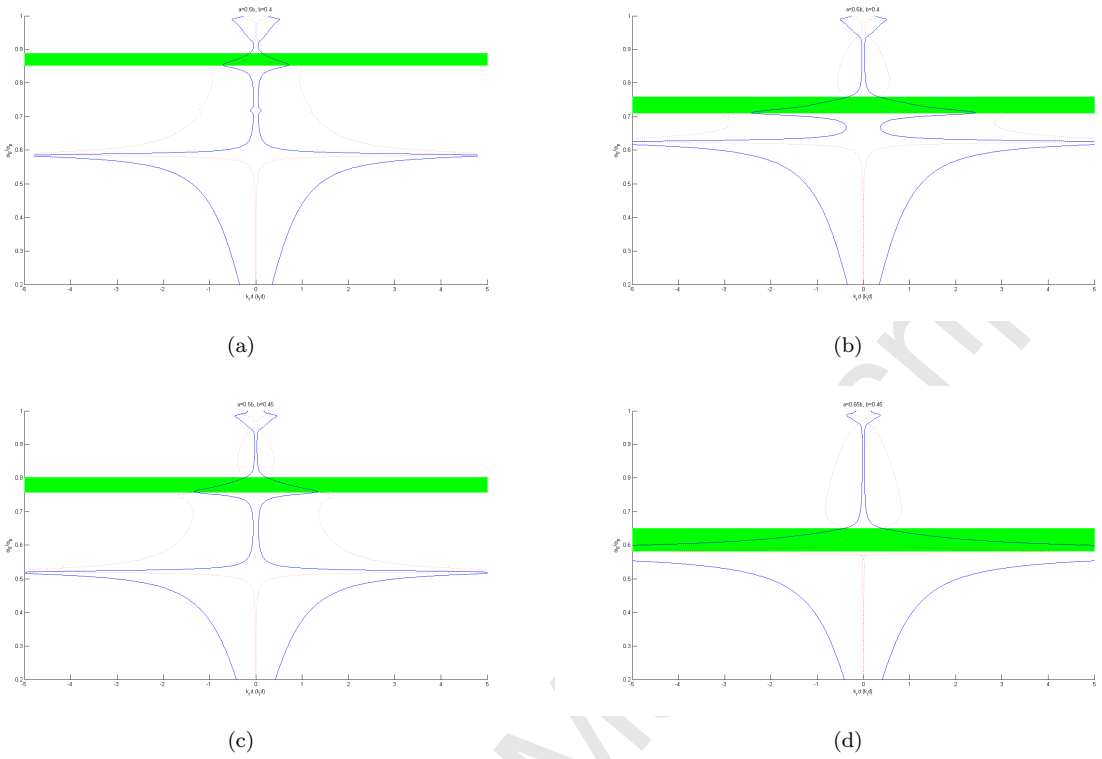

(a) (b)

(c) (d)

Figure 4: Dispersion curves associated with different choice of inner and outer radii for the coating, when $\epsilon_R = 200 + i5$ and $\omega_c/\omega_p = 0.01$. The dashed line corresponds to the imaginary part dk_i, the solid line corresponds to the real part dk_r. The green stip gives the interval where $Re(\mu_{eff})$ and $Re(\epsilon_{eff}^{-1}\hat{\kappa}\cdot\hat{\kappa})$ are both negative. (a) is for $a = 0.5b, b = 0.4$; (b) for $a = 0.6b, b = 0.4$; (c) for $a = 0.5b, b = 0.45$; (d) for $a = 0.65b, b = 0.45$.

Here ϕ_ϵ and ϕ_μ are the arguments of ϵ_{eff} and μ_{eff} respectively. They satisfy $0 \le \phi_\epsilon, \phi_\mu \le \pi$. Therefore $\phi_n \in [0, \pi]$. Then we find that

$$Re\left(\frac{\mu_{eff}}{n_{eff+}}\right) > 0 \text{ and } Re\left(\frac{\mu_{eff}}{n_{eff-}}\right) < 0. \tag{4.7}$$

Hence when $Re(n_{eff+}) < 0$ (and $Re(n_{eff-}) > 0$), (4.3) and (4.4) show that in the homogenization limit the energy flow and phase velocity are in opposite directions. $Re(n_{eff+}) < 0$ indicates that $\phi_n \in [\pi/2, \pi]$. Three cases should be considered: $(i)\frac{\pi}{2} \le \phi_\epsilon \le \pi, \pi - \phi_\epsilon \le \phi_\mu \le \frac{\pi}{2}$; $(ii)\frac{\pi}{2} \le \phi_\mu \le \pi, \pi - \phi_\mu \le \phi_\epsilon \le \frac{\pi}{2}$; $(iii)\frac{\pi}{2} \le \phi_\epsilon, \phi_\mu \le \pi$. Straightforward calculation shows that $Re(n_{eff+}) < 0$ is equivalent to the following inequality

$$\mu_r|\epsilon_{eff}| + \epsilon_r|\mu_{eff}| < 0. \tag{4.8}$$

We notice that if $\mu_r < 0$ and $\epsilon_r < 0$, then (4.8) holds. In other words, if $Re(\mu_{eff}) < 0$ and $Re(\epsilon_{eff}^{-1}\hat{\kappa}\cdot\hat{\kappa}) < 0$, then $Re(n_{eff+}) < 0$, hence in the homogenization limit the energy flow and phase velocity are in opposite directions. However it should remarked that $\mu_r < 0$ and $\epsilon_r < 0$ are not the necessary and sufficient condition for (4.8). That is, the frequency interval such that the phase velocity is opposite to the energy flow should be larger than the interval in which the real parts of μ_{eff} and $\epsilon_{eff}^{-1}\hat{\kappa}\cdot\hat{\kappa}$ are both negative.

5 Electrostatic resonances, plasmons, and Mie resonances

In what follows we describe the eigenvalue problems for the source free fields associated with electrostatic resonances (i.e., plasmon resonances) and Mie resonances. Here the Mie resonances are associated with the rod core and are precisely the eigenfunctions associated with the Dirichlet spectrum of the core cross section. While the electrostatic resonances are expressed by generalized source free fields permeating the rod coating and host. These resonances while not interacting directly control the physics of the dispersion relation to leading order by fixing the poles of the frequency dependent dielectric permittivity (electrostatic resonances) and the poles of the effective magnetic permeability (Dirichlet resonances). The first two terms in the power series expansion for the magnetic field ψ_0 and ψ_1 are expressed in terms of the eigenfunctions associated with these resonances. To start we write down the boundary value problems determining ψ_0 and ψ_1 obtained by equating like powers of the series expansion. The first term ψ_0 solves the following problem outside the rod core R on the domain $Y \setminus R$ given by

$$-\nabla_{\mathbf{y}} \cdot \left(a_0^{-1}(\mathbf{y}) \nabla_{\mathbf{y}} \psi_0(\mathbf{y})\right) = 0 \quad \text{in } Y \setminus R \tag{5.1}$$

with $n \cdot \nabla_{\mathbf{y}} \psi_0 = 0$ on the boundary of R. Here $a_0^{-1} = 1$ in the host and $a_0^{-1} = \epsilon_P^{-1}(\xi_0 k)$ in the coating. Equation (5.1) is an electrostatic resonance problem associated with a period cell containing a coated rod with core of infinite dielectric constant immersed in a host of unit dielectric constant. As written it appears to depend on the material properties of the coating. However we follow [12], [11] to see that it can be written as an equivalent electrostatic spectral problem depending only on the periodic coated rod configuration. The eigenpairs $\psi_{\lambda_n}, \lambda_n$ for the electrostatic problem depend only on geometry and are independent of the dielectric properties of the coating and solve the following electrostatic resonance problem intrinsic to the structure given by

$$\nabla_{\mathbf{y}} \cdot (\sigma(\mathbf{y}) \nabla_{\mathbf{y}} \psi_{\lambda_n}) = \lambda_n \Delta_{\mathbf{y}} \psi_{\lambda_n}, \text{ on } Y \setminus R, \tag{5.2}$$

with $n \cdot \nabla_{\mathbf{y}} \psi_{\lambda_n} = 0$ on the boundary of R and $\sigma = -1/2$ in the coating and $\sigma = 1/2$ in the host. It is shown in [12] that the only non-constant solutions of (5.1) are given by the plasmons ψ_{λ_n} and only when $\epsilon_P^{-1}(\xi_0 k) = (\lambda_n + 1/2)/(\lambda_n - 1/2)$. Hence we suppose that $\epsilon_P^{-1}(\xi_0 k) \neq (\lambda_n + 1/2)/(\lambda_n - 1/2)$ and we can choose $\psi_0 = 1$ for points inside $Y \setminus R$. The theory developed in [12] shows the generalized electrostatic spectra $\{\lambda_n\}$ lies in the open interval $(-1/2, 1/2)$ with zero being the only accumulation point. The plasmons $\{\psi_{\lambda_n}\}_{n=0}^{\infty}$ associated with the electrostatic resonances $\{\lambda_n\}_{n=1}^{\infty}$ form a complete orthonormal set of functions in the space of mean zero periodic functions belonging to $H^1_{per}(Y \setminus R)$ that are harmonic in P and H, [12]. Here orthonormality is with respect to the inner product $(u, v) = \int_{Y \setminus R} \nabla u \cdot \nabla \overline{v} \, dx$. The complete orthonormal systems of eigenfunctions associated with electrostatic resonances and Dirichlet eigenvalues are used to solve for ψ_0 and ψ_1 in $H \cup P$. We follow [12] to find that

$$-\Delta \psi_0 = \gamma k^2 \xi_0^2 \psi_0, \text{ in } R \tag{5.3}$$

with $\psi_0 = 1$ on the boundary of R. We also find that ψ_1 is the solution of

$$-\Delta \psi_1 \quad = \quad 0, \text{ in } P \text{ and in } H \tag{5.4}$$

and the corresponding transmission conditions for ψ_1 are given by

$$n \cdot (\nabla \psi_1 + \hat{\kappa})_{|_H} \quad = \quad n \cdot \epsilon_P^{-1}(\xi_0 k) \, (\nabla \psi_1 + \hat{\kappa})_{|_P}, \text{ H-P interface,} \tag{5.5}$$

$$n \cdot \epsilon_P^{-1}(\xi_0 k) \, (\nabla \psi_1 + \hat{\kappa})_{|_P} \quad = \quad 0, \text{ R-P interface.} \tag{5.6}$$

Expanding ψ_1 in terms of the complete set of orthonormal eigenfunctions $\{\psi_{\lambda_n}\}$ we obtain the the representation

$$\psi_1 = - \sum_{-1/2 < \lambda_n < 1/2} \left(\frac{(\alpha^1_{\lambda_n} + \epsilon_P^{-1}(\xi_0 k) \alpha^2_{\lambda_n})}{1 + (\epsilon_P^{-1}(\xi_0 k) - 1)(\frac{1}{2} - \lambda_n)} \right) \psi_{\lambda_n}, \text{ in } Y \setminus R \tag{5.7}$$

with

$$\alpha^1_{\lambda_n} = \hat{\kappa} \cdot \int_H \nabla \psi_{\lambda_n}\, d\mathbf{y}, \quad \text{and } \alpha^2_{\lambda_n} = \hat{\kappa} \cdot \int_P \nabla \psi_{\lambda_n}\, d\mathbf{y}. \tag{5.8}$$

A straight forward calculation gives ψ_0 in R in terms of the complete set of Dirichlet eigenfunctions and eigenvalues $\{\mu_n\}$ and $\{\phi_n\}$:

$$\psi_0 = \sum_{n=1}^{\infty} \frac{\mu_n < \phi_n >_R}{\mu_n - \gamma k^2 \xi_0^2} \phi_n, \text{ in } R, \text{ with} \tag{5.9}$$

$$< \phi_n >_R = \int_R \phi_n \, d\mathbf{y}. \tag{5.10}$$

6 Acknowledgments

This research is supported by AFOSR MURI Grant FA9550-12-1-0489 administered through the University of New Mexico and by NSF grant DMS-1211066.

References

[1] A. Alu and N. Engheta, *Dynamical theory of artifical optical magnetism produced by rings of plasmonic nanoparticles,* Phys. Rev. B, 78 (2008), 085112.

[2] A. Alu, A.D. Yaghjian, R.A. Shore, and M.G. Silveirinha, *Causality relations in the homogenization of metamaterials,* Phys. Rev. B, 84 (2011), 054305.

[3] A. Alu, *First principles homogenization theory for periodic metamaterial arrays,* Phys. Rev. B, 84 (2011), 075153.

[4] D. J. Bergman, *The dielectric constant of a simple cubic array of identical spheres,* Journal of Physics C: Solid State Physics, 12 (1979), pp.4947–4960.

[5] C. F. Bohren and D.H.Huffman, *Absorption and Scattering of Light by Small Particles,* Wiley, 2004.

[6] G. Bouchitté and C. Bourel, *Homogenization of finite metallic fibers and 3D-effective permittivity tensor,* Commun. Comput. Phys., (2010) To appear.

[7] G. Bouchitté and B. Schweizer, *Homogenization of Maxwell's equations in a split ring geometry,* Multiscale Model. Simul., 8 (2010), pp. 717–750.

[8] G. Bouchitté and D. Felbacq, *Negative refraction in periodic and random photonic crystals,* New J. Phys., 7 (2005), 159.

[9] G. Bouchitté and D. Felbacq, *Homogenization near resonances and artificial magnetism from dielectrics,* C. R. Acad. Sci. Paris I, 339 (2004), PP. 377–382.

[10] O. P. Bruno, *The effective conductivity of strongly heterogeneous composites,* Proceedings of the Royal Society of London, A,433 (1991), pp. 353–381.

[11] Y. Chen and R. Lipton, *Double Negative Dispersion Relations from Coated Plasmonic Rods,* SIAM, Multiscale Modeling and Simulation, (2013), in press; arXiv:1202.0602 [math.AP] 3 Feb 2012.

[12] Y. Chen and R. Lipton, *Resonance and double negative behavior in metamaterials,* Archive for Rational Mechanics and Analysis, (2013), accepted for publication March 4, 2013; arXiv:1111.3586v1 [math.AP] 15 Nov 2011.

[13] Y. Chen and R. Lipton, *Tunable double negative band structure from non-magnetic coated rods,* New J. Phys., 12 (2010), 083010.

[14] R. L. Chern and D. Felbacq, *Artificial magnetism and anticrossing interaction in photonic crystals and split-ring structures,* Phys. Rev. B, 79 (2009), 075118.

[15] G. Dolling, C. Enrich, M. Wegener, C. M. Soukoulis and S. Linden, *Low-loss negative-index metamaterial at telecommunication wavelengths,* Opt. Lett., 31 (2006), PP. 1800–1802.

[16] D. Felbacq and G. Bouchitté, *Homogenization of wire mesh photonic crystals embdedded in a medium with a negative permeability,* Phys. Rev. Lett., 94 (2005), 183902.

[17] S. P. Fortes, R. P. Lipton and S. P. Shipman, *Sub-wavelength plasmonic crystals: dispersion relations and effective properties,* Proc. R. Soc. Lond. Ser. A, 466 (2009), pp. 1993–2020.

[18] S. P. Fortes, R. P. Lipton and S. P. Shipman, *Convergent power series for fields in positive or negative high-contrast periodic media,* Comm. Partial Differential Equations, 36 (2011), pp. 1016–1043.

[19] J. Huangfu, L. Ran, H. Chen, X. Zhang, K. Chen, T. M. Grzegorczyk and J. A. Kong, *Experimental confirmation of negative refractive index of a metamaterial composed of Ω-like metallic patterns,* Appl. Phys. Lett., 84 (2004), 1537.

[20] K. C. Huang, M. L. Povinelli and J. D. Joannopoulos, *Negative effective permeability in polaritonic photonic crystals,* Appl. Phys. Lett., 85 (2004), 543.

[21] R. Kohn and S. Shipman, *Magnetism and homogenization of micro- resonators,* Multiscale Model. Simul., 7 (2008), pp. 62–92.

[22] R. C. McPhedran, N. A. Nicorovici, L. C. Botten and A. B. Movchan, *Advances in the Rayleigh multipole method for problems in photonics and phononics,* in IUTAM Symposium on Mechanical and Electromagnetic Waves in Structured Media, R.C. McPhedran, ed., Kluwer Academic Publishers, 2001, pp. 15–28.

[23] R. C. McPhedran and G. W. Milton, *Bounds and exact theories for the transport properties of inhomogeneous media,* Applied Physics A, 26 (1981), pp. 207–220.

[24] A. Mejdoubi and C. Brosseau, *Intrinsic resonant behavior of metamaterials by finite element calculations,* Physical Review B, 74 (2006), 165424.

[25] G. W. Milton, *The Theory of Composites*, Cambrige University Press, Cambridge UK, 2002.

[26] G. W. Milton, *Realizability of metamaterials with prescribed electric permittivity and magnetic permeability tensors,* New J. Phys. 12 (2010), 033035.

[27] N. A. Nicorovici, R. C. McPhedran and G. W. Milton, *Transport properties of a 3 phase composite material: the square array of coated cylinders,* Proc. R. Soc. Lond. Ser. A, 422 (1993), pp. 599–620.

[28] J. Pendry, A. Holden, D. Robbins and W. Stewart, *Magnetisim from conductors and enhanced nonlinear phenomena,* IEEE Trans. Microw. Theory Tech., 47 (1999), pp. 2075–2084.

[29] J. Pendry, A. Holden, D. Robbins and W. Stewart, *Low frequency plasmons in thin-wire structures,* J. Phys.: Condens. Matter, 10 (1998), pp. 4785–4809.

[30] L. Peng, L. Ran, H. Chen, H. Zhang, L. A. Kong and T. M. Grzegorczyk, *Experimental observation of left-handed behavior in an array of standard dielectric resonators,* Phys. Rev. Lett., 98 (2007), 157403.

[31] W. T. Perrins, D.R. Mckenzie and R. C. McPhedran, *Transport properties of regular arrays of cylinders,* Proc. R. Soc. Lond. Ser. A, 369 (1979), pp. 207–225.

[32] R. F. Service, *Next Wave of metamaterials hopes to fuel the revolution,* Sci., 327 (2010), pp. 138–139.

[33] V. Shalaev, *Optical negative-index metamaterials,* Nature Photonics, 1 (2007), pp. 41-48.

[34] V. M. Shalaev, W. Cai, U. K. Chettiar, H. K. Yuan, A. K. Sarychev, V. P. Drachev, and A. V. Kildishev, *Negative index of refraction in optical metamaterials,* Opt. Lett., 30 (2005), pp. 3356–3358.

[35] R. A. Shelby, D. R. Smith and S. Schultz, *Experimental verification of a negative index of refraction,* Sci., 292 (2001), pp. 77–79.

[36] S. Shipman, *Power series for waves in micro-resonator arrays,* in Proceedings of the 13th International Conference on Mathematical Methods in Electrodynamic Theory, Kyiv, Ukraine: IEEE, 2010.

[37] G. Shvets and Y. Urzhumov, *Engineering the electromagnetic prop- erties of periodic nanostructures using electrostatic resonances,* Phys. Rev. Lett., 93 (2004), 243902-1-4.

[38] D. R. Smith and J. B. Pendry, *Homogenization of metamaterials by field averaging,* J. Opt. Soc. Amer. B, 23 (2006), pp. 391–403.

[39] D. R. Smith, W. Padilla, D. Vier, S. Nemat-Nasser and S. Schultz, *Composite medium with simultaneously negative permeability and permittivity,* Phys. Rev. Lett., 84 (2000), pp. 4184–4187.

[40] J. W. Strutt, *On the influence of obstacles arranged in rectangular order upon the properties of a medium* Phil. Mag., 34 (1892), pp. 481–502.

[41] V. G. Veselago, *The electrodynamics of substances with simultaneously negative values of ϵ and μ,* Sov. Phys. Usp., 10 (1968), 509.

[42] K. Vynck, D. Felbacq, E. Centeno, A. I. Cabuz, D. Cassagne and B. Guizal, *All-dielectric rod-type metamaterials at optical frequencies* Phys. Rev. Lett., 102 (2009), 133901.

[43] M. S. Wheeler, J. S. Aitchison and M. Mojahedi, *Coated non-magnetic spheres with a negative index of refraction at infrared frequencies,* Phys. Rev. B, 73 (2006), 045105.

[44] V. Yannopapas, *Negative refractive index in the near-UV from Au-coated CuCl nanoparticle superlattices,* Phys. Stat. Sol. (RRL), 1 (2007), pp. 208–210.

[45] V. Yannopapas, *Artificial magnetism and negative refractive index in three-dimensional metamaterials of spherical particles at near-infrared and visible frequencies,* Appl. Phys. A, 87 (2007), pp. 259–264.

[46] F. Zhang, S. Potet, J. Carbonell, E.Lheurette, O. Vanbesien, X. Zhao and D. Lippens, *Negative-zero-positive refractive index in a prism-like omega-type metamaterial,* IEEE Trans. Microw. Theory Tech., 56 (2008), 2566.

[47] S. Zhang, W. Fan, B. K. Minhas, A. Frauenglass, K. J. Malloy and S. R. J. Brueck, *Midinfrared resonant magnetic nanostructures exhibiting a negative permeability,* Phys. Rev. Lett., 94 (2005), 037402.

[48] X. Zhou and X. P. Zhao, *Resonant condition of unitary dendritic structure with overlapping negative permittivity and permeability,* Appl. Phys. Lett., 91 (2007), 181908.